Eur. Phys. J. A **26**, 221–225 (2005)
DOI 10.1140/epja/i2005-10176-1

THE EUROPEAN PHYSICAL JOURNAL A

A theoretical description of energy spectra and two-neutron separation energies for neutron-rich zirconium isotopes

J.E. García-Ramos[1,a], K. Heyde[2], R. Fossion[2], V. Hellemans[2], and S. De Baerdemacker[2]

[1] Departamento de Física Aplicada, Universidad de Huelva, 21071 Huelva, Spain
[2] Institute for Theoretical Physics, Vakgroep Subatomaire en Stralingsfysica, Proeftuinstraat 86, B-9000 Gent, Belgium

Received: 12 September 2005 / Revised version: 24 October 2005 /
Published online: 5 December 2005 –
Communicated by G. Orlandini

Abstract. Very recently the atomic masses of neutron-rich Zr isotopes, from ^{96}Zr to ^{104}Zr, have been measured with high precision. Using a schematic Interacting Boson Model (IBM) Hamiltonian, the evolution from spherical to deformed shapes along the chain of Zr isotopes, describing at the same time the excitation energies as well as the two-neutron separation energies, can be rather well reproduced. The interplay between phase transitions and configuration mixing of intruder excitations in this mass region is succinctly addressed.

PACS. 21.60.Fw Models based on group theory – 27.70.+q $150 \leq A \leq 189$

Nuclear masses and binding energies, or more in particular two-neutron separation energies (S_{2n}), form a very important observable that characterizes a given nucleus and supply information about nuclear correlations providing at the same time a stringent test for nuclear models.

The goal of this paper is to make use of a technique developed in ref. [1] in order to describe at the same time the energy spectra and S_{2n} values obtained from a very recent experimental study of masses for the neutron-rich Zr isotopes (see refs. [2,3]) and nearby Sr and Mo isotopes [4]. This transitional region is of particular interest because a rapid change in the structure of Zr isotopes from mass $A = 98$ onwards is observed, *i.e.* a rather sudden change from spherical to well-deformed shapes [5–7]. This region is known for the appearance of deformed intruder states that even become the ground state and initiate the onset of a region of deformed nuclei for the heavier Zr isotopes [8] (beyond $N = 58$). Therefore, a study has been attempted in order to analyze the experimental variation observed in S_{2n} values.

For a theoretical description of the Zr isotopes, encompassing both the low-lying excitations as well as the intruder states, one should be using a very large shell model configuration space using the corresponding effective nucleon-nucleon interaction [9]. An attempt in that respect has been carried out for ^{92}Zr [10] using a restricted model space considering both proton and neuron orbitals outside of a ^{88}Sr core nucleus. In view of the fact that besides neutrons filling the 50–82 shell one would need to consider protons in the 28–40 shell, including proton excitations into the $1g_{9/2}$ configuration, calculations would become unfeasible. Therefore, we start from a strongly truncated model space, however keeping the pairing and quadrupole force components within the Interacting Boson Model (IBM) approximation [11]. This model approximates the interacting many-fermion problem using as major degrees of freedom, N pairs of valence nucleons that are treated as bosons, carrying angular momentum either 0 (the s-bosons) or 2 (the d-bosons). This model is very appropriate in order to describe even-even medium-mass and heavy nuclei and transitional nuclei. Even here, treating proton and neutron bosons explicitly, one risks to be involved with too many model parameters. Therefore, in the present description of the Zr isotopes, we make use of an approach in which we restrict ourselves to the use of identical bosons. This act of truncation naturally implies that one has to replace the Hamiltonian by an effective IBM Hamiltonian describing the interactions amongst these identical bosons [12]. Our approach here is very similar to a recent study of the Pt nuclei [13], a region in which there exist clear indications of the presence of intruder excitations.

The IBM Hamiltonian used is composed of a single-boson energy term, a quadrupole and an angular-momentum term,

$$\hat{H} = \varepsilon_d \hat{n}_d - \kappa \hat{Q} \cdot \hat{Q} + \kappa' \hat{L} \cdot \hat{L}, \tag{1}$$

where $\hat{n}_d$ denotes the d-boson number operator and

$$\hat{L} = \sqrt{10}(d^\dagger \times \tilde{d})^{(1)}, \tag{2}$$

$$\hat{Q} = s^\dagger \tilde{d} + d^\dagger \tilde{s} + \chi(d^\dagger \times \tilde{d})^{(2)}. \tag{3}$$

[a] e-mail: enrique.ramos@dfaie.uhu.es

We point out that in more realistic calculations, the values $\varepsilon_d > 0$ and $\kappa > 0$ [14–18] have been used. Moreover, the $E2$ transition operator is taken to have the same structure of the quadrupole operator $\hat{Q}$ appearing in the Hamiltonian,

$$\hat{Q}(E2) = e_{eff}\hat{Q}. \tag{4}$$

This approach is known as the Consistent-Q Formalism (CQF) [19].

The definition of the two-neutron separation energies is the following (starting from the binding energies):

$$S_{2n} = BE(N) - BE(N-1), \tag{5}$$

where N denotes the number of valence nucleon pairs and it is assumed that we are treating nuclei belonging to the first half of the neutron shell (50–82) filling up with increasing mass number.

The Hamiltonian (1) generates the energy spectrum of each individual Zr nucleus and will be called "local Hamiltonian". For the correct description of binding energies, one needs to add that part of the Hamiltonian that does not affect the spectrum and that will be called "global Hamiltonian"(and so it depends on the total number of bosons only [1]). The simplest interpretation of the IBM global part comes from the fact that this part describes the overall smooth varying energy term and can be associated with the structure of the Liquid-Drop Model. Therefore, the description we use, within the context of the IBM, is somehow similar to the Strutinsky method [20,21] in the sense that the global part takes care of the major contribution to the nuclear binding energy BE, while the local part, that is notably smaller, modulates this global behavior and describes the local correlations. An alternative way to incorporate binding energy effects in the IBM results from explicitly taking into account the s-boson one-body contribution $\varepsilon_s\hat{n}_s$ and the s-boson two-body interaction energy $u_0 s^\dagger s^\dagger ss$. One can, however, eliminate these s-boson terms taking into account the conservation of the number of bosons, giving rise to terms proportional to N and $N(N-1)$ in the binding energies, while they are proportional to N in the two neutron separation energies (see ref. [22]). Thus, this procedure is equivalent to the method used here and in ref. [1].

The contribution of the global part of the Hamiltonian to the S_{2n} is expressed as

$$S_{2n}^{gl} = \mathcal{A} + \mathcal{B}N, \tag{6}$$

where $\mathcal{A}$ and $\mathcal{B}$ are assumed to be constant along a chain of isotopes (see [1]). Therefore,

$$S_{2n}(N) = \mathcal{A} + \mathcal{B}N + BE^{lo}(N) - BE^{lo}(N-1), \tag{7}$$

where BE^{lo} is the local binding energy derived from the Hamiltonian (1).

In order to obtain a global description of the Zr isotopes, we prefer to consider a reduced number of parameters, keeping the Hamiltonian (1) as constant as possible when passing from isotope to isotope. Because the heavier Zr isotopes exhibit energy spectra that are the more rotational, the ratios $E(4_1^+)/E(2_1^+)$ and $E(6_1^+)/E(2_1^+)$ are used for fixing the parameters of the Hamiltonian, while in the lighter and medium isotopes the energies of the 2_1^+, 2_2^+ and 0_2^+ states are used to fix the Hamiltonian. The fact that, in particular, for the 4_1^+ and 0_2^+ states, large deviations appear when comparing the calculated $B(E2)$ values with the experimental data (see also table 2), points out that large contributions of configurations outside of the purely collective IBM model space are present in those states. This effect is enhanced for the low number of bosons present in the lighter isotopes. Thus, even though we cannot describe nuclear excited-state properties in detail for the light Zr nuclei, what is, however, more relevant in the present study is the important change in the low-lying energy spectra when passing from mass $A = 98$ towards mass $A = 100$ that is reproduced rather well. This is also essential in deriving the binding energy effects and the S_{2n} values.

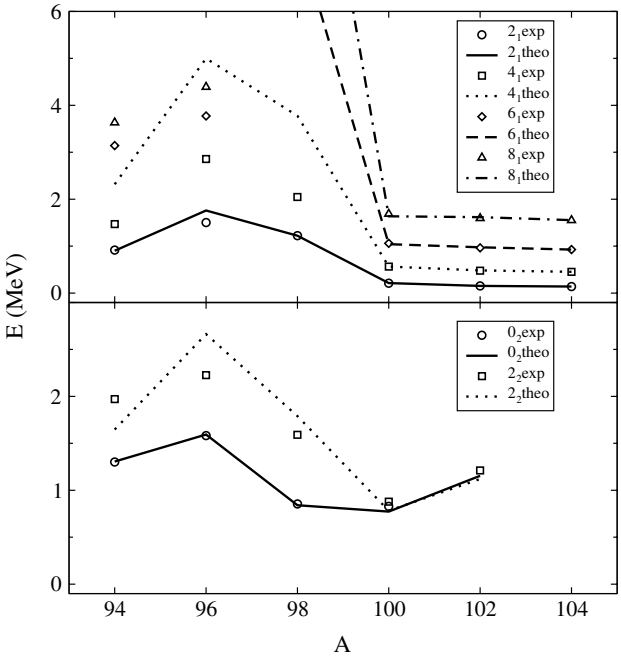

Fig. 1. Comparison between the theoretical and experimental energy levels (refs. [23–28]) for the neutron-rich Zr isotopes.

The experimental data for the different Zr isotopes have been taken from refs. [23–30]. Note that in this region, one expects the presence of intruder states but, as discussed before, those excitations are outside of the model space and are absorbed within an effective way within the changing parameters of the Hamiltonian (1) we are using in the present study. Therefore, the intruder states should be identified but not considered explicitly in the fitting procedure; this is the main difference with the technique used in ref. [13], where the intruder states are considered in the fitting procedure. The more clear-cut examples, in this region, where extra configuration and thus mixing will appear, are ^{98}Zr and ^{100}Zr [6,31,32]. In ^{98}Zr the 0_3^+ state at 1.436 MeV is supposed to form the head of an intruder band [33]. This then could induce mixing between the 4^+

Table 1. Parameters, describing the IBM Hamiltonian of eq. (1), for the Zr isotopes.

A	94	96	98	100	102	104
N	2	3	4	5	6	7
ε_d	0.550	0.750	0.380	0.311	0.211	0.213
κ	0.032	0.032	0.032	0.032	0.046	0.046
χ	-0.8	-0.8	-0.8	-0.8	-0.8	-0.8
κ'	0.05	0.17	0.15	0	0	0

states resulting in pushing down the 4_1^+ state, whose energy is indeed overestimated by the IBM calculation (see fig. 1). In the case of ^{100}Zr, the 0_2^+ state at 0.331 MeV is considered as an intruder state, while the 0_3^+ state at 0.829 MeV is considered to be the regular state. Therefore, in fig. 1, the 0^+ state that is plotted is indeed the state 0_3^+. Information on the characteristics of the excited 0^+ states in these nuclei is gained by studying $E0$ properties as discussed in detail by Wood *et al.* [7]. Note that in fig. 1 the theoretical states for the lighter isotopes with angular momenta 6 and 8 stay out of scale, which shows again the influence of the intruder states in the lower part of the spectra. An additional problem in the description of this region arises from the low number of bosons we should use, in other words because of the proximity of the shell closure for neutrons. This creates two inconveniences; on the one hand it is difficult to give a reasonable description for high angular momentum (note that the maximum angular momentum one can construct coupling IBM bosons is the double of the number of bosons) as observed recently in ^{96}Sr and ^{98}Zr nuclei [34] and, on the other hand, in the spectrum there appears non-collective excitation that can only be described by a shell model calculation (see, *e.g.*, [10]).

There is a very poor knowledge of $E2$ transition rates in this mass region and so it is difficult to fix the value of parameter χ because its value it is not well defined using the information about energy spectra only. Therefore, its value is fixed taking into account the information from other calculations addressing nuclei in nearby mass regions [18].

In the present calculations, we count bosons starting from a $Z = 40, N = 50$ core ^{90}Zr which has a rather high-lying first-excited state. This is at variance with recent shell model calculations for this mass region [10] that start from a $^{88}_{38}\mathrm{Sr}_{50}$ core. Since we make use of the interacting boson model approach (IBM) that does not discriminate between proton and neutron bosons, collective properties are mainly governed by the symmetry structure of the IBM Hamiltonian and the total number of bosons present. Using proton and neutron boson degrees of freedom, in a more detailed IBM study, one needs both proton and neutron bosons to be active in order for collective deformation effects to appear. This then would imply a different choice of a closed proton core, conform with the shell model.

The parameters of the Hamiltonian are summarized in table 1. Here, one notices that χ is fixed at the value of -0.8. The values of κ are restricted to 0.032 MeV for the Zr nuclei situated in the spherical and transitional region and to 0.046 MeV for the Zr nuclei exhibiting rotational-like energy spectra in the ground band. Note the high value of ε_d in the case of ^{96}Zr which is due to the abnormally high excitation energy of the 0_2^+ state that is described in terms of a subshell closure at the neutron $N = 56$.

Table 2. Comparison between experimental and theoretical $B(E2)$ values. The parameters of the quadrupole operator are $e_{eff} = 0.159$ eb and $\chi = -0.8$.

Isotope	Transition	$B(E2)$ ($\mathrm{e^2b^2}$) Exp.	$B(E2)$ ($\mathrm{e^2b^2}$) Theo.
^{94}Zr	$2_1^+ \to 0_1^+$	0.013	0.053
^{94}Zr	$4_1^+ \to 2_1^+$	0.002	0.027
^{94}Zr	$0_2^+ \to 2_1^+$	0.370	0.037
^{96}Zr	$2_1^+ \to 0_1^+$	0.010	0.088
^{100}Zr	$2_1^+ \to 0_1^+$	0.226	0.226
^{100}Zr	$8_1^+ \to 6_1^+$	0.336	0.251
^{102}Zr	$2_1^+ \to 0_1^+$	0.297	0.347

We present in table 2 the comparison between the experimental and theoretical $E2$ transition rates, keeping $\chi = -0.8$ and fixing $e_{eff} = 0.159$ eb for reproducing the $B(E2; 2_1^+ \to 0_1^+)$ value in ^{100}Zr. The agreement of the results is reasonable except for the transitions $4_1^+ \to 2_1^+$ and $0_2^+ \to 2_1^+$ in ^{94}Zr, which suggests that those states are outside of the IBM collective space to a large extent, as is also corroborated by the shell model calculations carried out in ^{92}Zr [10]. The 4_3^+ state located at 2.330 MeV is a good candidate as IBM partner, while there is no other candidate for the 0^+ state.

Once the energy spectra for the even-even Zr isotopes have been fitted, one derives the global part of S_{2n} (6) assuming the equivalence

$$S_{2n}^{gl} \equiv \mathcal{A} + \mathcal{B}N = S_{2n}^{exp} - S_{2n}^{lo}. \tag{8}$$

Note that the left-hand side of eq. (8) can be written in terms of the atomic number, A, through a trivial transformation in the parameters $\mathcal{A}$ and $\mathcal{B}$. In practice, the right-hand side of eq. (8) is not an exact relation but results approximately in a straight line. As a consequence the linear part is derived from a best fit to the data points, obtained when plotting the right-hand side of (8). We like to stress at this point (see also ref. [1]) that both the results concerning relative energies (energy spectra) and the energy surfaces do not depend on the values of $\mathcal{A}$ and $\mathcal{B}$ as determined here.

The global part of S_{2n} corresponds to the values $\mathcal{A} = 67.4$ MeV and $\mathcal{B} = -0.946$ MeV (using the atomic number, A, as variable). The comparison between the experimental data and the theoretical results, combining the global and the local part, is given in fig. 2. We like to point out that the approximately flat behavior of S_{2n} at $A = 100, 102$ is rather well reproduced and corresponds

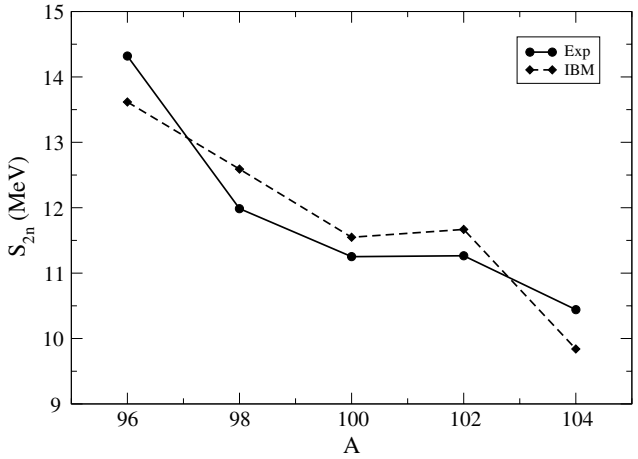

Fig. 2. Two-neutron separation energies for neutron-rich Zr isotopes. Full lines correspond to experimental data [2], while dashed lines correspond to theoretical calculations.

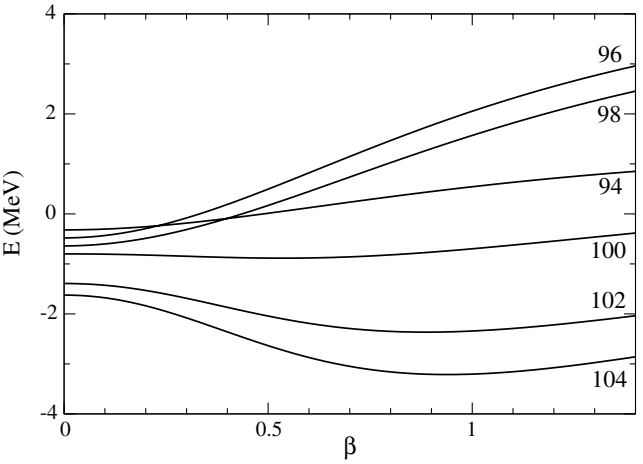

Fig. 3. Energy surfaces for Zr isotopes using the IBM intrinsic-state formalism. The number on each curve denotes the atomic mass number.

precisely to the neutron number where the energy spectra rapidly change from spherical into deformed structures.

Extra information that can be obtained from the present IBM calculation is the energy surface as a function of the deformation parameters. This can most easily be studied using the intrinsic-frame formalism. Here, the interacting many-boson problem is solved defining a new kind of boson —dressed bosons— that is built as a linear combination of s and d bosons and constructing a trial wave function as a condensate of N such bosons [35,36]. The problem is solved by minimizing the expectation value of the Hamiltonian with respect to the deformation parameters, that reduces to only one, β. In fig. 3, we present the energy surfaces for the different Zr isotopes according to the parametrization as described in table 1. It is clearly observed that $^{94-98}$Zr remain spherical. Note that the flat energy surface of ^{94}Zr appears due to the low number of bosons for this nucleus, $N = 2$, and to the fact that the depth of the potential energy surface is proportional to $N(N-1)$. ^{100}Zr is a special case because this nucleus appears to be situated very close to the critical region where two minima coexist [37], one spherical and one deformed. One notices that the energy surface is very flat, which is caused by the fact that a deformed minimum and a spherical maximum appear, that are almost degenerate. This indicates that one is close to the critical area [37] Finally, $^{102-104}$Zr become well deformed. Recent theoretical studies using relativistic mean-field (RMF) methods [38] (concentrating mainly on nuclear charge radii) and Hartree-Fock-Bogoliubov (HFB) methods [39] (studying the Zr isotopic chain up to the two-neutron drip line) have concentrated on shape properties and their variation from spherical towards strongly deformed Zr nuclei.

In this brief report, we have studied the energy spectra and the S_{2n} values for the neutron-rich even-even Zr isotopes in a consistent way using the IBM framework. The new experimental data on masses are rather well reproduced starting from a schematic calculation. From inspecting the corresponding energy surface diagrams, one clearly observes how the Zr isotopes evolve from spherical into deformed shapes passing through a region where two minima exist. The calculations that have been carried out imply the possible presence of a phase transition, being ^{98}Zr an almost critical nucleus. On the other hand, this mass region can also be described using configuration mixing (this will be shown elsewhere) in such a way that for ^{98}Zr, regular and intruder states coexist very closely in energy although it should be necessary to see if the S_{2n} values can be appropriately described. Both descriptions can seem equivalent, but there exist clear differences [40] in the size of the model spaces. In the calculations carried out here, the model space only consists of states with N bosons and we can follow the sequence of all states within this space as a function of the boson number and a smoothly changing Hamiltonian (see eq. (1) and table 1). On the other hand, when treating the presence of intruder states explicitly, one has to expand the configuration space such that both N and $N+2$ boson configurations are considered. It might be that the occurrence of the deformed states as lowest states, forming the ground-state band from ^{100}Zr onwards, can be associated with an adiabatic crossing of the more deformed ($N+2$ boson) configurations and the more spherical (N boson) configurations [8]. A microscopic origin can then be related with the possibility of exciting protons from the $2p_{1/2}$ into the $1g_{9/2}$ orbital and the subsequent large proton-neutron interaction energy gain with the neutron $1g_{7/2}, 1h_{11/2}$ orbitals beyond $N = 58$ [41–44]. Clearly, more work needs to be carried out in order to see if there exist mass regions where phase transitions are induced by the presence of low-lying intruding configurations and the corresponding configuration mixing.

The authors are grateful to J. Äystö for interesting discussions. This work has been partially supported by the Spanish DGI under project No. FPA2003-05958. Financial support from the "FWO-Vlaanderen" (K.H. and V.H.), the University of Gent (S.D.B. and K.H.) and the IWT (R.F.) as well as from the OSTC (Grant IUAP # P5/07) is also acknowledged.

References

1. R. Fossion, C. De Coster, J.E. García-Ramos, T. Werner, K. Heyde, Nucl. Phys. A **697**, 703 (2002).
2. S. Rinta-Antila *et al.*, Phys. Rev. C **70**, 011301(R) (2004).
3. G. Audi, A.H. Wapstra, C. Thibault, Nucl. Phys. A **729**, 337 (2003).
4. U. Hager *et al.*, private communication.
5. P. Möller, J.R. Nix, At. Data Nucl. Data Tables **26**, 165 (1981).
6. K. Heyde, J. Moreau, M. Waroquier, Phys. Rev. C **29**, 1859 (1984).
7. J.L. Wood, E.F. Zganjar, C. De Coster, K. Heyde, Nucl. Phys. A **651**, 323 (1999).
8. K. Heyde, J. Jolie, J. Moreau, J. Ryckebusch, M. Waroquier, P. Van Duppen, M. Huyse, J.L. Wood, Nucl. Phys. A **466**, 189 (1987).
9. E. Caurier, G. Martínez-Pinedo, F. Nowacki, A. Poves, A.P. Zuker, Rev. Mod. Phys. **77**, 427 (2005).
10. C. Fransen *et al.*, Phys. Rev. C **71**, 054304 (2005).
11. F. Iachello, A. Arima, *The Interacting Boson Model* (Cambridge University Press, Cambridge, 1987).
12. K. Heyde, *Basic Ideas and Concepts in Nuclear Physics* Ser. Fundam. Appl. Nucl. Phys., 3rd edition (Institute of Physics, Bristol, Philadelphia, 2004).
13. E.A. McCutchan, R.F. Casten, N.V. Zamfir, Phys. Rev. C **71**, 061301 (2005).
14. O. Scholten, F. Iachello, A. Arima, Ann. Phys. (N.Y.) **115**, 325 (1978).
15. O. Scholten, PhD Thesis, University of Groningen (1980).
16. J. Stachel, P. Van Isacker, K. Heyde, Phys. Rev. C **25**, 650 (1982).
17. R.F. Casten, J.A. Cizewki, Nucl. Phys. **309**, 477 (1978).
18. W.-T. Chou, N.V. Zamfir, R.F. Casten, Phys. Rev. C **56**, 829 (1997).
19. R.F. Casten, D.D. Warner, Rev. Mod. Phys. **60**, 389 (1988).
20. V.M. Strutinsky, Nucl. Phys. A **95**, 420 (1967).
21. V.M. Strutinsky, Nucl. Phys. A **122**, 1 (1968).
22. See page 12 of ref. [11].
23. J.K. Tuli, Nucl. Data Sheets **66**, 1 (1992).
24. M.R. Bhat, Nucl. Data Sheets **82**, 547 (1997).
25. B. Singh, Z. Hu, Nucl. Data Sheets **98**, 547 (2003).
26. B. Singh, Nucl. Data Sheets **81**, 1 (1997).
27. D. De Frenne, E. Jacobs, Nucl. Data Sheets **83**, 535 (1998).
28. J. Blachot, Nucl. Data Sheets **64**, 1 (1991).
29. H. Mach, E.K. Warburton, W. Krips, R.L. Gill, M. Moszynski, Phys. Rev. C **42**, 568 (1990).
30. D. Pantelica *et al.*, Phys. Rev. C **72**, 024304 (2005).
31. K. Heyde, R.A. Meyer, Phys. Rev. C **37**, 2170 (1988).
32. C. De Coster, K. Heyde, B. Decroix, J.L. Wood, J. Jolie, H. Lehmann, Nucl. Phys. A **651**, 31 (1999).
33. G. Lhersonneau *et al.*, Phys. Rev. C **49**, 1379 (1994).
34. C.Y. Wu *et al.*, Phys. Rev. C **70**, 064312 (2004).
35. A.E.L. Dieperink, O. Scholten, F. Iachello, Phys. Rev. Lett. **44**, 1747 (1980).
36. J.N. Ginocchio, M.W. Kirson, Nucl. Phys. A **350**, 31 (1980).
37. F. Iachello, Phys. Rev. Lett. **85**, 3580 (2000); **87**, 052502 (2001); **91**, 132502 (2003).
38. M. Hemalatha, A. Bhagwat, A. Shirivastava, S. Kailas, Y.K. Gambhir, Phys. Rev. C **70**, 044320 (2004).
39. A. Blazkiewicz, V.E. Oberacker, A.S. Umar, M. Stoitsov, Phys. Rev. C **70**, 054321 (2005).
40. K. Heyde, J. Jolie, R. Fossion, S. De Baerdemacker, V. Hellemans, Phys. Rev. C **69**, 054303 (2004).
41. P. Federman, S. Pittel, Phys. Lett. B **69**, 385 (1977).
42. P. Federman, S. Pittel, Phys. Rev. C **20**, 820 (1979).
43. A. Etchegoyan *et al.*, Phys. Rev. C **39**, 1130 (1989).
44. E. Kirchuck *et al.*, Phys. Rev. C **47**, 567 (1993).